2.4 Effective Storm-Relative Helicity in Supercell Thunderstorm Environments

Richard L. Thompson*, Roger Edwards, and Corey M. Mead
Storm Prediction Center
Norman, OK

1. Introduction

Since its introduction in the late 1980s and early 1990s, storm-relative helicity (e.g., Davies-Jones et al. 1990) has received widespread acceptance within the operational forecasting community as a supercell and tornado forecast parameter. Predictive estimates of storm-relative helicity (hereafter SRH) have relied on various storm motion algorithms (most recently Bunkers et al. 2000) and approximations of the storm "inflow layer" depth (typically the lowest 1-3 km above ground level). In an attempt to refine the estimates of the storm inflow layer, the depth of the layer is constrained by the vertical profiles of temperatures and moisture. Specifically, it is assumed that only lifted parcels associated with positive buoyancy will sustain a thunderstorm updraft, whereas parcels associated with large convective inhibition will ultimately result in storm demise. Magnitudes of 100 J kg^{-1}, 250 J kg^{-1}, and 500 J kg^{-1} for CAPE (after Doswell and Rasmussen 1994) and convective inhibition (CIN) were tested as potential thresholds for determining storm inflow depth for the "effective" SRH. The tests were performed by beginning at the ground level in the sounding and searching upward for the first lifted parcel to satisfy the CAPE and CIN constraints, and this level was designated the "effective base". Continuing upward from the effective base, each level in a sounding was examined until either of the CAPE or CIN constraints were violated, and this level was designated the "effective top" of the inflow layer. The vertical distance between these two levels defines the effective storm inflow layer.

* Corresponding author address: Richard L. Thompson, 1313 Halley Circle, Norman, OK 73069. Email: Richard.thompson@noaa.gov

2. Data and Methodology

The RUC model close proximity sounding sample described in Thompson et al. (2003; hereafter T03) has been expanded to include storm cases from 2003 and 2004, increasing the sample size to 916 soundings. In a slight change from the T03 methodology, we collected soundings for both the initiation and mature phases of supercells, as described in Edwards et al. (2004). However, to remain consistent with T03, we considered only a single mature phase sounding for each storm case, or an initiation sounding if no mature phase sounding was collected for a particular storm.

An illustration of the effective layer technique is provided in Fig. 1. The skew-t log P sounding plotted is the RUC-2 model close proximity sounding for an elevated right-moving supercell case from May 2001. The dark horizontal lines across the temperature and moisture profile, marked at 900 hPa and 650 hPa, denote the base and top of the effective inflow layer, based on a

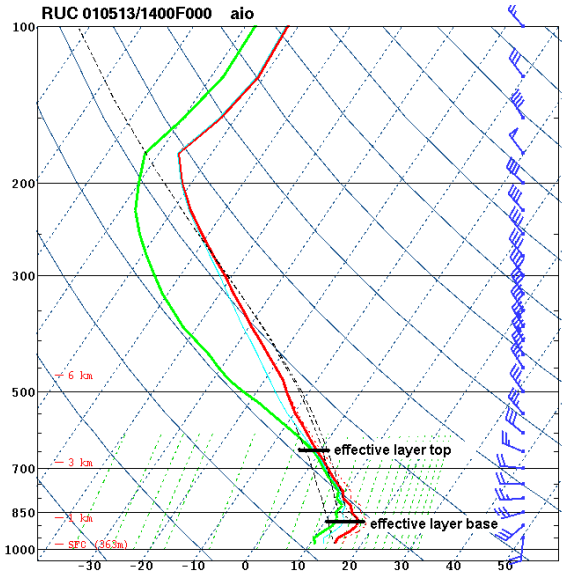

Figure 1. Skew-t/log P plot of a RUC-2 model proximity sounding for an elevated right-moving supercell. The heavy horizontal lines marked on the temperature and moisture profiles denote the locations of the "effective base" (near 900 hPa) and the "effective top" (near 650 hPa), using parcel constraints of 100 J kg-1 CAPE and -250 J kg-1 CIN.

parcel CAPE > 100 J kg^{-1} and a parcel CIN > -250 J kg^{-1}. For these CAPE and CIN constraints, the effective inflow layer in Fig. 1 begins at 699 m above model ground level, and extends upward to 3395 m above model ground level, resulting in an inflow layer depth of 2696 m. The same technique was applied to all 916 close proximity soundings derived from the RUC model, utilizing CAPE and CIN magnitude thresholds of 100 J kg^{-1}, 250 J kg^{-1} and 500 J kg^{-1}.

As part of this investigation, it became necessary to develop a storm motion technique that applies to both surface-based and elevated supercells. The "internal dynamics (ID) method" supercell motion algorithm developed by Bunkers et al. (2000) relies on estimating two components of storm motion: advection by the mean wind, and storm propagation based on the vector shear through a portion of the storm depth. Each of these components were examined by Bunkers et al. (2000), and storm motion errors were minimized for the mean wind and vector shear through the lowest 6 km above ground level layer. However, all of the supercells in the Bunkers data set were surface based, which brings into question the utility of the ID method in elevated supercell cases where the supercells can be decoupled vertically from the near-ground environment.

To account for the possibility of a storm decoupled from the near-ground environment, the ID method was modified to include the "effective shear" described in Thompson et al. (2004a), as well as the mean wind through the same layer as the effective shear. A simple test of this modified ID method was performed on our sample of 95 significantly tornadic (F2 or greater damage) supercell soundings, and 39 elevated right-moving supercell soundings. A comparison of mean absolute errors for the ID method and the modified ID method revealed error reductions of 0.09 m s^{-1} and 0.51 m s^{-1} for the significantly tornadic (surface-based) supercells and elevated supercells, respectively, when using the modified ID method.

3. Results

The ranges of median heights for the top and base of the effective storm inflow layer are shown in Fig 2. The variation of the CIN constraint from -250 J kg^{-1} to -500 J kg^{-1} has little impact on the effective layer depth for all storm groups (compare the red and gray bars in Fig. 2), likely because CIN magnitudes greater than 250 J kg^{-1} are rare in this proximity sounding sample. Variation of the CAPE from 100 J kg^{-1} to 500 J kg^{-1} has a larger impact and tends to reduce the depth of the effective layer by several hundred meters (compare the blue

bars to the gray bars in Fig. 2). It is important to note that the most stringent constraints (500 J kg^{-1} CAPE and -250 J kg^{-1} CIN) resulted in the loss of storm soundings when no parcels in the profile met the constraints. The number of soundings with no parcels meeting the most stringent constraints (primarily the CAPE constraint) ranged from 25% of the elevated right-movers, to 7% of the non-supercells, to only 1% of the significantly tornadic supercells.

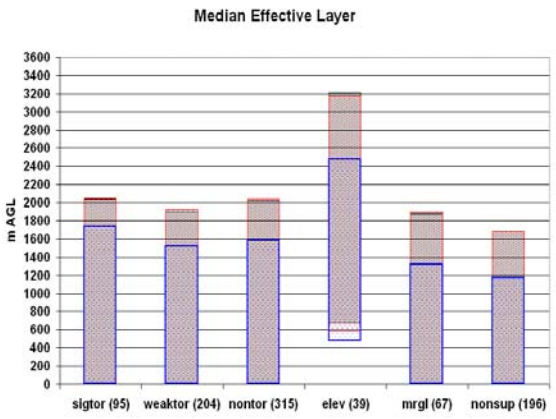

Figure 2. Median effective layer depths (m above ground level) for proximity soundings associated with six classes of thunderstorms with sample sizes noted in parentheses on the figure: significantly tornadic supercells (sigtor), weakly tornadic supercells (weaktor), nontornadic supercells (nontor), elevated right-moving supercells (elev), marginal right-moving supercells (mrgl), and discrete nonsupercells. The top of each bar represents the median effective layer top, and the bottom of the bars represent the median effective layer base. The solid gray bars are for the 100 J kg^{-1} CAPE and -250 J kg^{-1} CIN parcel constraints, the light red bars are for the 100 J kg^{-1} CAPE and -500 J kg^{-1} CIN parcel constraints, and the heavier blue outlined bars are for the 500 J kg^{-1} CAPE and -500 J kg^{-1} CIN parcel constraints.

Figure 3 shows the depth of the effective inflow layer varies linearly with the threshold choices such that the deepest effective layers correspond to the least stringent CAPE and CIN thresholds (e.g., CAPE > 100 J kg^{-1} and CIN > -500 J kg^{-1}) and the shallowest effective layers correspond to the most stringent thresholds (CAPE > 500 J kg^{-1} and CIN > -250 J kg^{-1}). The least stringent effective layer constraints (CAPE > 100 J kg^{-1} and CIN > -500 J kg^{-1}) result in inflow layer depths typically ranging from 1 to 3 km above ground level, though there is substantial variability from case to case.

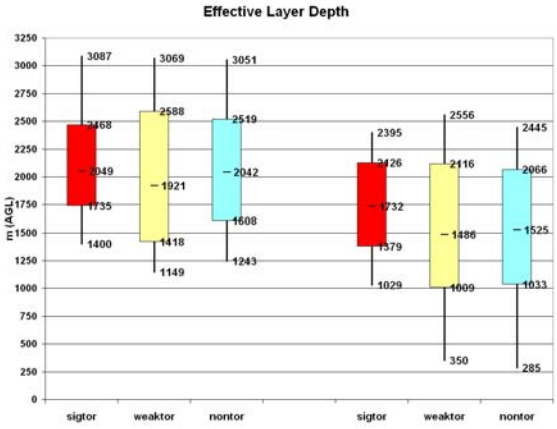

Figure 3. Box and whiskers plots of effective layer depth (m above ground level) for the less stringent 100 J kg^{-1} CAPE and -500 J kg^{-1} CIN parcel constraints on the left, and the more stringent 500 J kg^{-1} CAPE and -250 J kg^{-1} CIN parcel constraints on the right. The shaded boxes denote the range of values from the 25th to the 75th percentiles, with the median values labeled within the box. The whiskers extend upward to the 90th percentile values, and downward to the 10th percentile values. The supercell groups shown and sample sizes are the same as in Fig. 2.

Effective SRH decreases markedly from the significantly tornadic supercells to the nontornadic supercells (Fig. 4), while the effective SRH with elevated right-moving supercells (which rarely produce tornadoes themselves) resembles the values associated with nontornadic supercells. The ability to discriminate between significantly tornadic, weakly tornadic, and nontornadic supercells with SRH based on the effective layer is not particularly sensitive to the specific threshold choices tested. Since almost all of

our RUC model proximity soundings contained parcels that met the minimum 100 J kg^{-1} CAPE and -250 J kg^{-1} CIN constraints, these values were chosen to define the effective layer depth in the default effective SRH calculations.

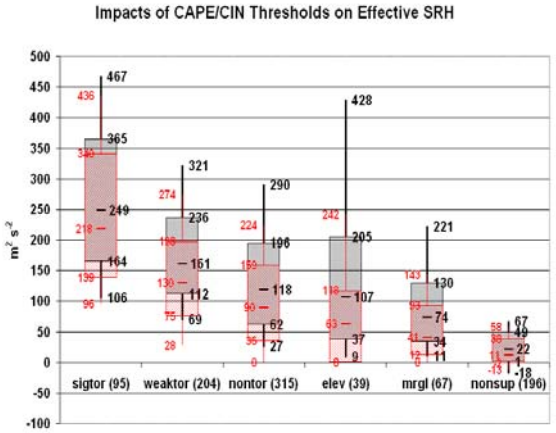

Figure 4. Box and whiskers overlay plots of effective SRH (m^2 s^{-2}) for each storm group corresponding to the most stringent parcel constraints in light red, and the least stringent parcel constraints in solid gray. The box and whiskers conventions are the same as Fig. 3, and the storm group conventions are the same as Fig. 2.

Calculations of SRH in supercell environments have been based typically on a fixed layer (e.g., 0-3 km above ground level) and a storm motion estimate that was developed from a sample of surface-based supercells (e.g., the ID method). Two concerns with this typical approach are the representativeness of 0-3 km as the "inflow" layer for most supercells, and the special case of over-estimating SRH in elevated supercell cases by including vertical shear in the near-ground layer that may be decoupled vertically from the storm (i.e., instability based above a stable surface layer in a warm advection pattern). The depth of the layer feeding a supercell updraft varies depending on the CAPE and CIN constraints chosen. For the particular default parcel constraints of at least 100 J kg^{-1} CAPE and a CIN magnitude of no more than 250 J kg^{-1} CIN, the depth of the inflow layer for the surface-based supercells varies from 1 km to 3 km above ground level (similar to the left hand side of Fig. 3). The median inflow layer depth for the elevated supercells is similar to that of the surface-based supercells, except that the effective storm base begins near 700 m above ground level (see Fig. 2).

In comparing SRH calculations for the effective inflow layers and the fixed 0-3 km layer (Fig 5), the effective SRH discriminates more clearly between the classes of surface-based supercells. The parcel constraints of 100 J kg^{-1} CAPE and -250 J kg^{-1} CIN are not so harsh as to mask elevated supercell environments with relatively small CAPE, but are substantial enough to remove the influence of inflow parcels characterized by either excessive CIN or minimal buoyancy.

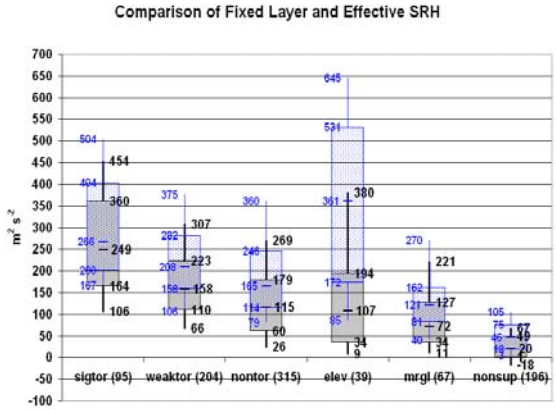

Figure 5. Box and whiskers overlay plots of effective SRH (m^2 s^{-2}) based on the 100 J kg^{-1} CAPE and -250 J kg^{-1} CIN parcel constraints (solid gray), and 0-3 km SRH (blue, m^2 s^{-2}). Storm group conventions are the same as Fig. 2.

Of particular interest in Fig. 5 is the large variation in SRH between the fixed 0-3 km layer and the effective layer for the elevated right-moving supercells. The other five storm groups reveal a consistent reduction in SRH from the 0-3 km layer to the effective

layer, owing to the shallower depth of the effective layer in the majority of cases (refer to Fig. 2). However, the impact of the effective layer is most pronounced with the elevated right-moving supercells, where 0-3 km SRH magnitudes are several times larger than the effective SRH values. Elevated supercells are relatively common in warm advection regimes which are associated with substantial CAPE based above the ground. The fixed 0-3 km layer includes the impact of the near-ground layer which tends to be characterized by large vertical shear but little or no buoyancy in these regimes. However, the effective SRH only considers the layer associated with some buoyancy and without excessive CIN. Results are similar when comparing the 0-1 km SRH to the effective SRH (Fig. 6).

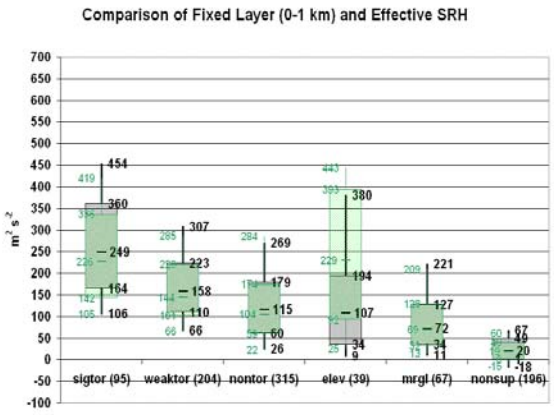

Figure 6. Same as Fig. 5, except with an overlay of the 0-1 km SRH (green).

An illustration of the impact of the effective layer approach on SRH calculations is shown in Fig. 7 for an elevated right-moving supercell case. The fixed layer 0-3 km SRH for this supercell case was 458 m^2 s^{-2} (ID Method storm motion), while the effective SRH was reduced to 158 m^2 s^{-2} (modified ID Method storm motion). The reduction in SRH owes to the exclusion of the relatively dry and stable layer from the ground to 900 hPa (see Fig. 1) in the effective SRH calculation.

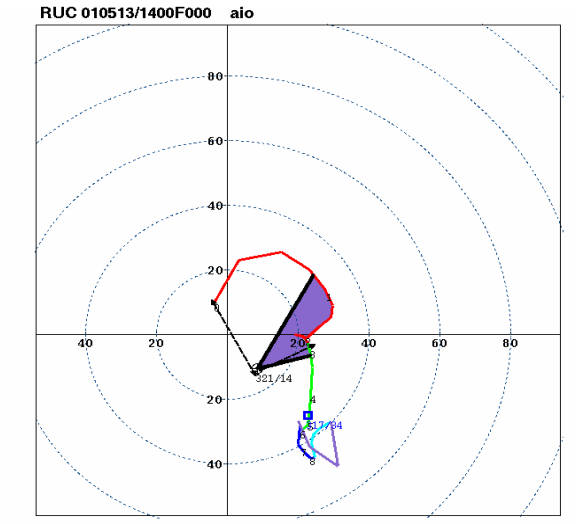

Figure 7. Hodograph illustration of the effective SRH for the same elevated supercell case presented in Fig. 1. The shaded area on the hodograph denotes the effective SRH layer, based on the modified ID method storm motion, and the dashed lines enclose the standard 0-3 km SRH area based on the ID method storm motion. The color coded segments of the hodograph represent the lowest 3 km (red), 3-6 km above ground level (green), 6-9 km above ground level (cyan), etc.

4. Conclusions

A technique to define the inflow layer of a thunderstorm, in terms of constraints on lifted parcel CAPE and CIN values, was developed and tested on a sample of 916 close proximity soundings derived from RUC model analyses, after T03. This sounding technique, identified as the effective layer, was applied to calculations of SRH with the intent of replacing fixed layer SRH calculations. Results of this approach suggest that the effective SRH more clearly discriminates between significantly tornadic and nontornadic supercells than the standard 0-1 km and 0-3 km fixed layer versions of SRH (see Rasmussen and Blanchard 1998), and is more representative of an elevated storm's available streamwise vorticity.

The effective inflow layer also allows calculation of a more meaningful storm-relative helicity for elevated thunderstorms by omitting layers in a sounding that are unlikely to contribute to storm updraft maintenance through either excessive CIN or insufficient CAPE. Our results suggest that the effective SRH (based on a parcel CAPE greater than 100 J kg^{-1} and less than a 250 J kg^{-1} CIN magnitude) can be used to identify environments favoring both surface-based and elevated right-moving supercells. Additionally, the effective SRH appears to be a more robust parameter that is worthy of inclusion in composite indices such as the Supercell Composite Parameter and Significant Tornado Parameter developed by T03, and updated by Thompson et al. (2004b).

5. Acknowledgments

Thanks goes to Steve Weiss for a thorough review of this work, and to the Science Support Branch for providing the authors with data access and storage. We also thank John Hart for his assistance in modifying the original NSHARP sounding code, and Lou Wicker for stimulating discussions in the early stages of this work.

6. References

Bunkers, M. J., B. A. Klimowski, J. W. Zeitler, R. L. Thompson, and M. L. Weisman, 2000: Predicting supercell motion using a new hodograph technique. *Wea. Forecasting*, **15**, 61-79.

Davies-Jones, R. P., D. W. Burgess, and M. Foster, 1990: Test of helicity as a tornado forecast parameter. Preprints, *16th Conf. on Severe Local Storms*, Kananaskis Park, AB, Canada, Amer. Meteor. Soc., 588-592.

Doswell, C. A. III, and E. N. Rasmussen, 1994: The effect of neglecting the virtual temperature correction on CAPE calculations. *Wea. Forecasting*, **9**, 625-629.

Edwards, R., R. L. Thompson, and C. M. Mead, 2004: Assessment of anticyclonic supercell environments using close proximity soundings from the RUC model. Preprints, *22nd Conf. on Severe Local Storms*, Hyannis, MA, Amer. Meteor. Soc. (this volume).

Rasmussen, E. N., and D. O. Blanchard, 1998: A baseline climatology of sounding-derived supercell and tornado parameters. *Wea. Forecasting*, **13**, 1148-1164.

Thompson, R. L., C. M. Mead, and R. Edwards, 2004a: Effective bulk shear in supercell thunderstorm environments. Preprints, *22nd Conf. on Severe Local Storms*, Hyannis, MA, Amer. Meteor. Soc. (this volume).

_____, R. Edwards, and C. M. Mead, 2004b: An update to the Supercell Composite and Significant Tornado Parameters. Preprints, *22nd Conf. on Severe Local Storms*, Hyannis, MA, Amer. Meteor. Soc. (this volume).

_____, _____, J. A. Hart, K. L. Elmore, and P. Markowski, 2003: Close proximity soundings within supercell environments obtained from the Rapid Update Cycle. *Wea. Forecasting*, **18**, 1243-1261.